Creep of Silicon Nitride with Neodymium and Yttrium Additions

Cosme Roberto Moreira da Silva(a), cosmeroberto@gmail.com
Claudinei dos Santos (b), claudinei@demar.faenquil.br
Flaminio Levy Neto (a) flaminio@unb.br

.
(a) Universidade de Brasília - Campus Universitário Darcy Ribeiro- Brasília –DF – CEP 70910 -900
(b) Faculdade de Engenharia Química de Lorena – Polo Urbo-Industrial S/N[0] – Gleba 16 – Lorena – SP –CEP 12600-000.

1 – Abstract

Silicon nitride samples were evaluated under compressive creep conditions, over a stress range of 50-300 MPa and temperature range of 1250 – 1400 ^{0}C. Si_3N_4 powders were mixed to neodymium and yttrium oxides and hot uniaxially pressed. Short term compressive creep behavior was evaluated in argon, followed by microstructural analysis by X-ray diffractometry and Transmission Electron Microscopy. Stress exponents near to unity were obtained for lower stress and temperature testing, suggesting grain boundary diffusion accommodation processes. Higher temperatures and stresses changed prevalent creep mechanism to cavitation, showing strong correlation of deformation processes with degree of crystallization and amount of intergranular phase.

2 – Introduction

Silicon nitride is considered as a strong candidate for fabrication of high efficiency turbine components, considering its low thermal expansion and high thermal-shock resistance [1]. Its thermal expansion coefficient is around $2.9 \times 10^{-6} < \alpha < 3.6 \times 10^{-6}$ K^{-1} for $20 < T < 1500$ ^{0}C [1,3]. In each of its structural modifications, α and β, silicon nitride has a unique combination of properties. It is strong, hard, wear resistant and stable to higher than 1800 ^{0}C [2]. The use of silicon nitride in turbine components would lead to weight savings and an increase in their operating temperatures, which would in turn increase fuel efficiency. The covalent character of the Si-N bonds and the extremely low self-diffusion coefficients of silicon and nitrogen increase the difficulty to sinter Si_3N_4. Sintering aids must be added to promote liquid phase sintering in such a way to achieve appropriate densification. During sintering, additives will react with silicon nitride and native SiO_2 on Si_3N_4 particles surfaces. The subsequent formation of the liquid oxinitride phase promotes particle rearrangement, $\alpha – Si_3N_4$ solution and subsequent $\beta – Si_3N_4$ reprecipitation, leading to densification. The intergranular phase formation is strongly important to the final high temperature properties [4]. Good densification has been achieved using yttrium oxide as sintering aid [5-8].

Lanthanide oxides are also strong candidates additives, taking into account their relatively high melting points, providing therefore highly refractory remnant amorphous grain boundary phase after sintering. The formed liquid intergranular phase originated from rare-earth sintering aids have high nitrogen content, high viscosity and glass transition temperature, which can improve substantially high temperature mechanical properties [10].

Creep formation occurs at high temperature when the amorphous grain boundary phase softens, thus permitting relative motion of the grains. Improvement of the refractoriness and reduction of the amount of the sintering aids have dramatically improved the creep resistance of silicon nitride [9]. The approach to improve its mechanical properties at elevated temperature by crystallization of grain boundary phases has also been demonstrated by several researchers [10-12].

Creep of silicon nitride based ceramics has been extensively tested in tension and bending [13-17]. A comprehensive review on Creep Mechanism in Multiphase Ceramic Materials [18] shows that only few researchers performed tests in those materials under compressive stress. Tests atmospheres in these cases were basically air [8,19-22].

The aim of the present investigation is to evaluate short term compressive creep behavior of Gas-Pressure sintered silicon nitride with neodymium/yttrium oxides mixtures as sintering aids. Creep tests were performed in argon, in temperature range of 1250 – 1400 ^{0}C and stress range of 50-300 MPa. High temperature creep mechanisms and stress exponent values are correlated to microstructural features observed by TEM and its relationship with the amount and composition of sintering aids and degree of crystallization of grain boundary phase.

3. Experimental Procedures

Commercial silicon nitride powder (SNE-10, UBE, Japan) was used for sample fabrication. Yttrium oxide (H.C. Stark, fine grade) and neodymium oxide (99.99 %, purity, Johnson Matthey Co., U.K.) were utilized as densification aids. The following steps were used for Y_2O_3/Nd_2O_3 powder mixture fabrication: The two powders (1:1 mol) were at first mixed in polypropylene containers during 24 hours, using dry ethanol as dispersing agent. The obtained fluid was dried, milled and heated up to 1000 ^{0}C, remaining at this temperature for three hours. The resulting product was milled during 24 hours, to obtain the adequate particle size distribution, for the sintering step.

Wet milling of silicon nitride and sintering aids during 48 hours in dry ethanol was used to produce samples of two different compositions (% in weight):

Composition A: 92 % Si_3N_4 + 8% neodymium oxide.
Composition B: 92 % Si_3N_4 + 8% yttrium/neodymium oxides mixture.

The samples were uniaxial and isostatically cold pressed at 300 MPa, as cylinders with approximately 2.5 mm diameter and 5.0 mm high after sintering. Discs with 20.0 mm diameter and 3.0 mm high were also cold pressed and sintered under the same conditions, to allow x-ray difractometry analysis. The gas pressure sintering was performed at 1800 ^{0}C and 4 MPa of maximum gas pressure. X-ray diffractometry analysis was performed in each composition, using a Philips PW 1840 diffractometer with Cu-Kα radiation.

Thin foils for Transmission Electron Microscopy examinations were prepared by mechanical polishing and ion beam thinning. The TEM samples were cut parallel to the applied stress axis of the compressive crept samples. The microscope accelerating voltage was in a range of 120-300 KV.

The furnaces used in the rigs were standard molybdenum-wound furnaces PCA-10, produced by Metals Research Ltd., Cambridge. To monitor specimen temperature and control furnace temperature, 6% Rhodium-Platinum against 30% Rhodium-Platinum thermocouples were used. The compression of the specimen on creep testing was sensed and measured by a LVDT.

Each silicon nitride sample was at first measured and inserted between the two silicon carbide discs, previously positioned between the extremity of the loading bar and the base of the loading molybdenum support tube. The furnace was then lifted to a position where the top end of the connecting port could be clamped and sealed against the lower face of the top plate. A stable argon flux was introduced into the system, with a silicone oil bubble at the gas outlet line, giving necessary backpressure to the system. After these procedures, the chart recorder and the adjustment voltage regulator feeding the LVDT were switched on, the follower pin of the LVDT was positioned against the horizontal bar carried on the plunger and a time of thirty minutes was allowed before the loads were applied to the system, enabling the various parts of the rig to equilibrate before creep displacements were recorded. Tests stress range were 50-300 MPa and temperature range 1250 – 1400 ^{0}C.

4 – Experimental Results and Discussion

4.1 – Density

The materials A and B reached densities above 99% of theoretical.

4.2 – Crystalline phases of sintered samples.

The identified crystalline phases at composition A, after sintering, were β-Si_3N_4 (H), $Nd_4Si_3O_{12}$ (H), $Nd_2Si_3O_3N_4$ (T) and $Nd_{10}(SiO_4)_6$ (T) .For composition B, such phases after sintering were basically β – Si_3N_4 (H), $Y_2Si_3O_3N_4$ (T), $Y_2Si_2O_7$ (M) and Nd_2O_3 (H). For this composition, neodymium silicates were not detected.

4.3 – Creep Rates

Figures 1 and 2 shows, respectively, creep rates as function of stress, using logarithmic values, for compositions A and B at several temperature levels.
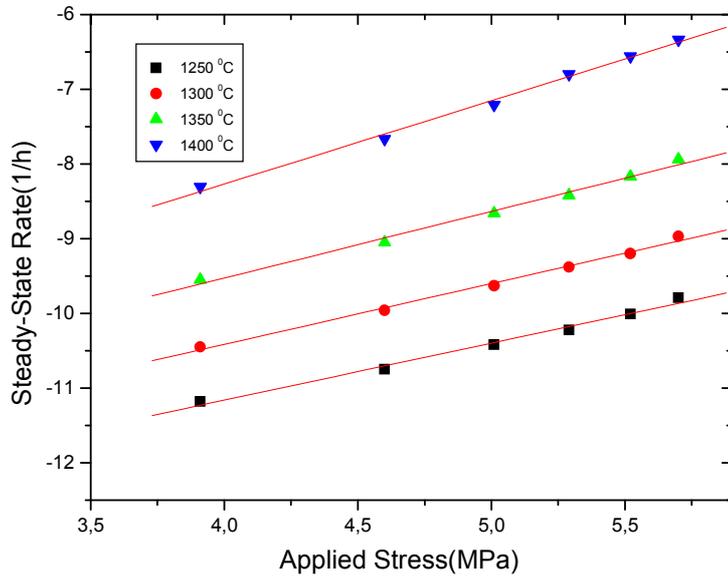
Figure 1 - Creep rates as function of applied stress, at different temperatures, for composition A
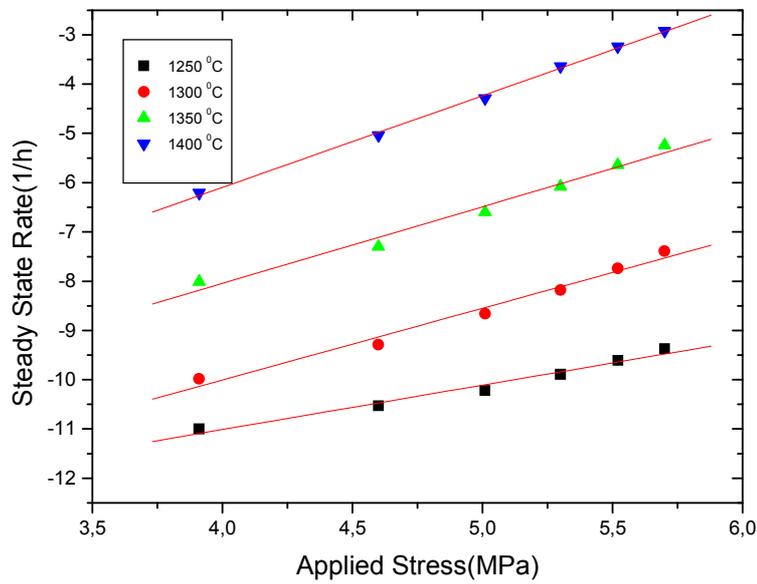

Figure 2 – Creep rates as function of applied stress, at different temperatures, for composition B.

The obtained creep rates for composition A were in a range between 0.75 and 1.10, indicative of diffusional creep predominance. Higher creep rates values were obtained for composition B, within a range from 0.89 and 1.87. Further MET examinations confirmed that cavitation would prevail, for higher temperature and stresses, in this case.

Estimates of creep activation energies were obtained from slopes of graphics at figures 1 and 2, giving a range of values between 630 and 660 KJ/mol for composition A and 790 and 810 KJ/mol for composition B.

Previous research (23) had already made correlation of heat of solution of silicon nitride and the intrinsic diffusivity and their contribution to the apparent activation energy for creep. The encountered values of activation energy for creep by solution-reprecipitation at that time are consistent with those of composition A.

Apparently a single thermally activated creep mechanism prevail at each stress level, for the composition with low A and high B previous glass phase contained.

4.4– Transmission Electron Microscopy

High Resolution Transmission Electron Microscopy has been used before for crept samples examination (1)(24)(25) in order to reveal the existing fine intergranular and multigrain junction glassy phase of silicon nitride ceramics with additive content. In the present work, energy dispersive microanalysis did not show evidence of neodymium or yttrium solubility in β–Si_3N_4 grains, and all the additions are retained at the silicate phase that involves the hexagonal β–Si_3N_4 (Figure 3). Amorphous and crystalline phases are retained at grain boundaries and multigrain junctions. A positive identification of the $Nd_2Si_3O_3N_4$ was made by a series of diffraction patterns (Figure 4). There is no evidence of dislocation activity at the examined samples, either for compositions A or B.

After being cooled under load at the end of creep test, the materials with low amount of glassy phase (A) did not show cavitation. It is considered (26) that existing asperities at grain boundaries were not smoothed out by diffusion, causing stress concentrations during sliding in which ledges of opposites signs lock, giving as a result a viscoelastic response of the material. Without sliding to load multigrain junctions, cavitation will not occur, and it may cause creep rate decrease. The unelastic recovery observed in some crept ceramic materials may be the unloading of strained, but uncavitated multigrain junctions.

Diffusional creep prevails as sliding accommodation for composition A, for all temperatures and stresses used in this work. The stress exponent near unity indicates in these cases local stresses acting as driving forces for the solution-reprecipitation mechanisms, controlled either by rate of reactions of solution-reprecipitation at the interface crystalline/glassy phase or by rate of transport trough intergranular phase. Cavities, mainly wedge-shaped, prevails for materials with higher anticipated glassy phase (B), under creep tests at and above 1350 ^{0}C (Figure 5). These discontinuities can be originated from pre-existing defects from the sintering process, or vapor bubbles which grows inside the glass during creep test, as can be seen at Figure 6, where such bubbles appears involving a grain of $Nd_2Si_3O_3N_4$ (N-melilite).
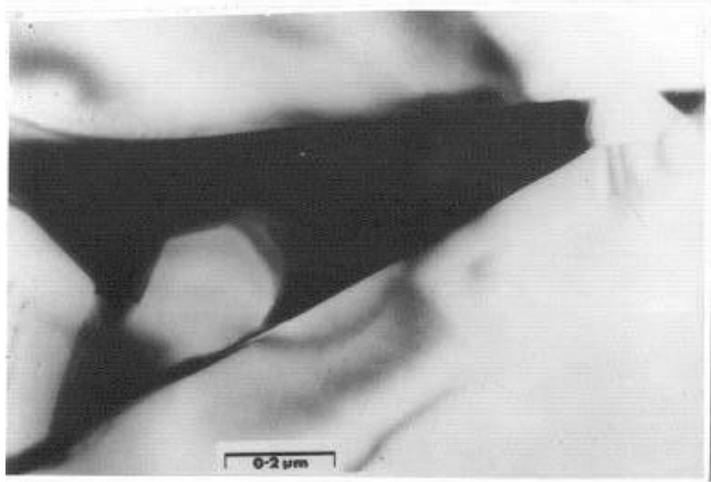
Figure 3 – N-Melilite phase (black area), at the hexagonal $\beta - Si_3N_4$ grain boundary phase.
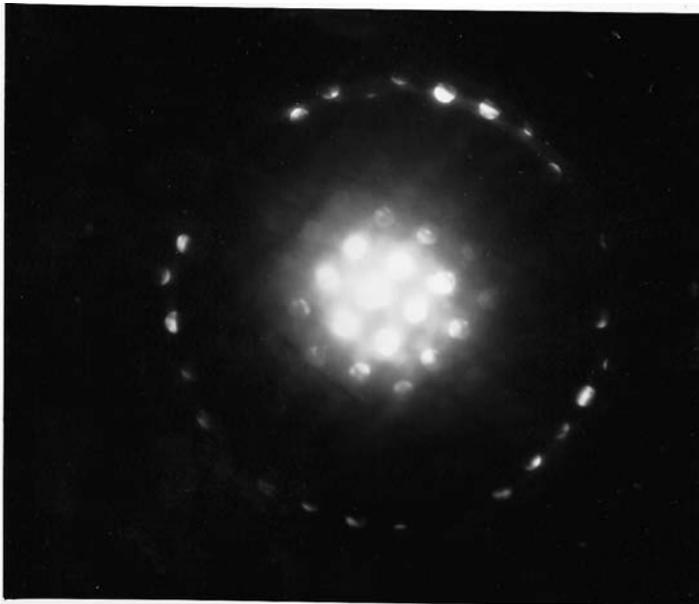

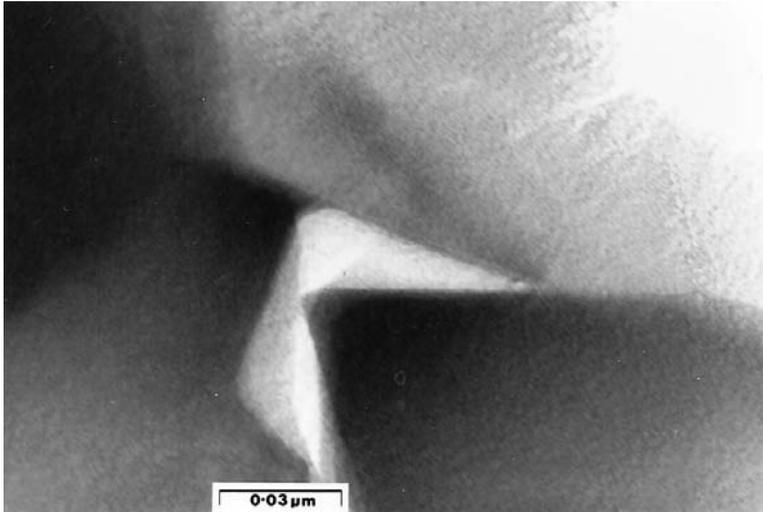Figure 4 – X-ray diffraction pattern of N-melilite phases

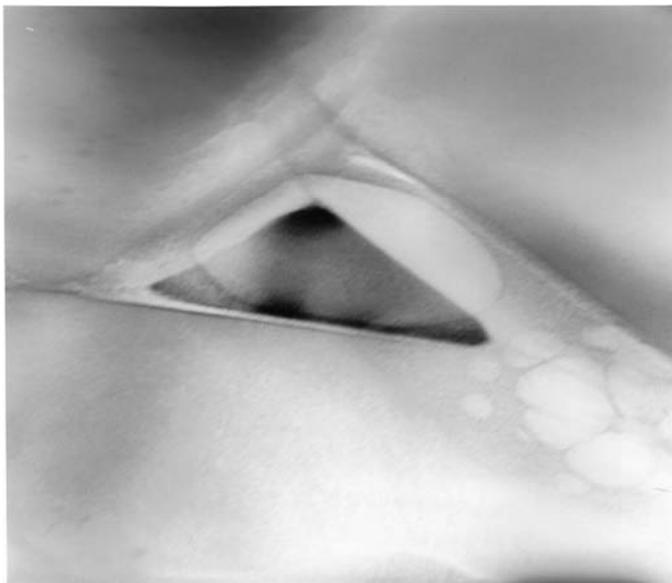Figure 5 – Wedge cracks on crept samples of composition B.

Figure 6 – Vapor bubbles at glass phase at grain junctions.

When diffusion does not prevail, viscous movement controlled by sliding rate of grain boundary can lead to elastic stress concentration at triple point junctions. The amount (extension) of sliding will be dependent upon volume and viscosity of the glassy phase at these regions. The growth of cavities in this situation would cause stress relaxation at triple point, allowing grain boundary sliding continuity. There is a progressive strain with subsequent cavity growth and new sliding.

The high number of wedge-cavities observed after creep test, at the composition with higher amount of glassy phase could be related to the higher probability of cavitation at thicker secondary glass phases at triple points. This higher probability is related to the higher surface energy for fracture originated from local compositional fluctuations (28). At higher sliding extension, prevalent for compositions with higher volume of intergranular glassy phase (B), the sliding overcomes the initial hydrostatic compression at silicate pockets. Cavities will form with subsequent flow of silicate, causing matter redistribution to surrounding pockets and, as a result, volume expansion. Grain boundary sliding will occurs to accommodate such expansion, causing loading at new multigrain pocket and cavitation creep. If load and temperature test conditions are high and amount and crystalline degree of intergranular phase are low in such a way that the accommodation process is not efficient, the growth of the cavities will proceed jacking the grains apart.

5 – Conclusions

For silicon nitride compositions with lower amount of intergranular glassy phases (8% neodymium) diffusional creep with sliding accommodation by diffusion species was predominant. In these cases, stress exponents values near unity indicates solution-reprecipitation mechanisms acting as driving forces , controlled either by rate of reactions of solution reprecipitation mechanisms, at the interface crystalline/glassy phase or by rate of transport trough intergranular phase. Cavitational creep was favored in situations where intergranular phase phase had greater thickness and lower viscosity. Wedge cavities, discernible by TEM, became prevalent with increase in amount and reduction of crystalline degree of the existing phase at grain boundary and multigrain junctions, for higher temperatures and stresses.

Cavities in fluids are dependent upon viscosity at the early stages (28). It is considered that the initial growth of wedge cracks at the associated model with the present work is initially restricted (constricted) by the grain boundary sliding.

6 – References

1 – Jin Q., Wilkinson D.S., and Weatherly G.C. , " Redistribution of a Grain Boundary Glass Phase During Creep of Si_3N_4 Ceramics", J. Am. Ceram. Soc., 79,211-14 (1996).

2 – Ralph F., Krause, J., Sheldon, J., Li Chien-Wei., "Tensile Creep Behaviour of a Gas-Pressure-Sintered Silicon Nitride Containing Silicon Carbide", J. Am. Ceram. Soc., 10, 2394-400 (2001).

3- K.M.Fox, J.R. Hellmann, E.C. Dickey, D.J. Green, D.L. Shellemn, ZR.L. Yeckley, [a] Impression and Compression Creep of SiAlON Ceramics[a] , J. Am. Ceram. Soc., 89, 2555 2563, (2006).

4 –Boling-Risser, M.A., Goretta, K.C., Routbort, J.L., Faber, K.T., "Effect of Miocrostructure on High Temperature Compressive Creep of Self-Reinforced Hot-Pressed Silicon Nitride", J. Am. Ceram. Soc., 83,3065-69 (2000).

5 – Saigalik P., Dusza J., and Hofman M.J., " Relationship Between Microstructure, Toughening Mechanisms, and Fracture Toughness of Reinforced Silicon Nitride Ceramics", J. Am. Ceram. Soc., 78 (10), 2619-24 (1995).

6 – Rendtel A., Hubner H., Herrmann M., Schubert C., " Silicon Nitride/ Silicon Carbide Nanocomposites Materials : II, Hot Strengh, Creep and Oxidation Resistance", J. Am. Ceram. Soc., 81, 1109-29 (1998).

7 – Rendtel A., Hubner H., Herrmann M., Schubert C., " Silicon Nitride/ Silicon Carbide Nanocomposites Materials: I , Fabrication and Mechanical Properties at Room Temperature", J. Am. Ceram. Soc., 81, 1095 -108 (1998).

8 – Crampon J., Duclos R., Peni F., Guicciardi S, De Portu. G., " Compressive Creep and Creep Failure of 8 $Y_2O_3/3Al_2O_3$ – Doped Hot Pressed Silicon Nitride", J. Am. Ceram. Soc., 80 (1) 85-91 (1997).

9 – Zhu S., Mizuno M. , Kagawa Y., "Creep Behaviour in SiC Reinforced Silicon Nitride Composite", J. of Mat. Sci., 34, 1799-07 (1999).

10 – Cinibulk M. K., Thomas G., Johnson S. M., "Fabrication and Secondary – Phase Crystallization of Rare-Earth Disilicate – Silicon Nitride Ceramics". J. Am. Ceram. Soc. 75 (8) 2037-43 (1992).

11 – Kerber M. K. and Genkins M. G., " Evaluation of The Strength and Creep Fatigue Behavior of Hot Isostatically Pressed Silicon Nitride", J. Am Ceram. Soc. 75 (9), 2543 – 62 (1992).

12 – Kerber M. K., Genkins M. G., Nolan T. A., Yeckley R. L., " Comparison of The Creep and Creep Rupture Performance of Two Hipped Silicon Nitride Ceramics", J. Am. Ceram. Soc., 779 (3) 657-65 (1994).

13 –William, L.E., "Results of an International Round-Robin for Tensile Creep Rupture of Silicon Nitride", J. Am. Cer. Soc., 85, 408-14 (2002).

14 – Hockley B. J., Widerhorn S.M., Liu W., Baldoni J. G. and Buljan S. T., " Tensile Creep of Whisker-Reinforced Silion Nitride", J. Mater. Sci., 26, 3931-39 (1991).

15 – Luecke, W., Widerhorn S. M., Hocley B.J. and Long G.G., " Cavity Formation During Tensile Creep of Si_3N_4", in Silicon Nitride Ceramics: Scientific and Technological Advances, Materials Research Society Symposium Proceedings, , Edited by Chen I-W, Becher P. F., Mitomo M., Petzow G. and Yen T. S., Materials Research Society, Pittsburgh, PA, 287, 467-72 (1993).

16 – Ohji T., Yamauchi Y. and Kanzaki S., " Tensile Creep and Creep Rupture Behavior of HIPed Silicon Nitride ", in Silicon Nitride, Edited by Hoffmann M., Petzow G. and Becher P. F., Trnas tech Aedermannsdorf, Switzerland, 92 (1993).

17 – Gasdaska C. J., "Tensile Creep in an In-Situ-Reinforced Silicon Nitride", J. Am. Ceram. Soc., 77, 208-18 (1994).

18 – Wilkinson D. S., " Creep Mechanism in Multiphase Ceramic Materials", J. Am. Ceram. Soc., 81 (2), 275-99 (1998).

19 – Ueke W. E., Wiederhorn S. M., Hockey B. J., Krause R. F., Long G. G., "Cavitation Contributes Substantially to Tensile Creep in Silicon Nitride", J. Am. Ceram. Soc., 78 (8) 2085-96 (1995).

20 – Julin Wan, Ren-Guan-Duan, Matthew J. G., Mukherjee A.K., "Highly Creep Resistant Silicon Nitride-Silicon Carbide Nano Composites" , J. Am. Cer. Soc. 89, 274 280 (2005).

21 – Ferber M. K., Jenkins M. G. and Tennery V. J., " Comparison of Tension, Compression and Flexure Creep for Alumina and Silicon Nitride Ceramics" , Ceram. Eng. Sci. Proc., 11(7) 1028-45 (1990).

22- Luecke W. and Wiederhorn S. M., " Tensile and Compressive Assymetry in Silicon Nitride", in Silicon Nitride '93. Edited by Hoffmann M., Petzow G. and Becher P. F., Trnas. Tech Aedermannsdorf, Switzerland, 587-91 (1993).

23 – Raj R. and Morgan P. E. D., " Activation Energies of Densification, Creep and Grain Boundary Sliding in Nitrogen Ceramics", J. Am. Ceram. Soc., 63, C-143-C-145 (1981).

24 - Braue W., Carpenter R. W., Smith D. J., " High-Resolution Interface Analysis of SiC-Whisker-Reinforced Si_3N_4 and Al_2O_3 Ceramic Matrix Composites" , J. Mater. Sci., 25, 2949-57 (1990).

25 – Falk L. K. L, Dunlop C. G. , " Crytallization of The Glassy Phase in a Si_3N_4 Material by Post-Sintering Heat Treatment", J. Mater. Sci., 22, 4369-76 (1987).

26 – Lange F. F. , Davis B. I. and Clarke D.R., " Compressive Creep of Si_3N_4/MgO Alloys: Part I, Effect of Composition", J. Mater. Sci., 15, 601-10 (1980).

27 – Raj R. and Chyung C. K., " Solution-Precipitation Creep in Glass Ceramics", Acta Metall., 29, 159-66 (1981).

28 – Clarke D. R., " The Intergranular Film in Silicon Nitride Ceramics – A Diffuse Interface Approach", pp 291-301 in Taloring of Mechanical Properties of Si_3N_4 Ceramics, Edited by Hofmann M. J., Kluwer, Dordrecht, The Netherlands, 1994.